Dynamics in the Plastic Crystalline Phase of Cyanocyclohexane and Isocyanocyclohexane Probed by ^{1}H Field Cycling NMR Relaxometry

Elisa Carignani[‡,†,*] *Max Flämig,*[§] *Lucia Calucci,*[‡,*] *Ernst A. Rössler*[§]

[‡] Istituto di Chimica dei Composti Organometallici - ICCOM, Consiglio Nazionale delle Ricerche - CNR, via G. Moruzzi 1, 56124 Pisa, Italy

[†] Dipartimento di Chimica e Chimica Industriale, Università di Pisa, via G. Moruzzi 13, 56124 Pisa, Italy

[§]Nordbayerisches NMR-Zentrum, Universität Bayreuth, 95440 Bayreuth, Germany

Corresponding Authors:

*Elisa Carignani, Istituto di Chimica dei Composti Organometallici (ICCOM), Consiglio Nazionale delle Ricerche (CNR), via G. Moruzzi 1, 56124 Pisa (Italy); Phone: +39 0503152433; E-mail:elisa.carignani@pi.iccom.cnr.it

*Lucia Calucci, Istituto di Chimica dei Composti Organometallici (ICCOM), Consiglio Nazionale delle Ricerche (CNR), via G. Moruzzi 1, 56124 Pisa (Italy); Phone: +39 0503152517; E-mail: lucia.calucci@pi.iccom.cnr.it.

ABSTRACT

Proton Field-Cycling NMR relaxometry is applied over a wide frequency and temperature range to get insight into the dynamic processes occurring in the plastically crystalline phase of the two isomers cyanocyclohexane (CNCH) and isocyanocyclohexane (iCNCH). Spin-lattice relaxation rate, $R_1(\omega)$, is measured in the 0.01-30 MHz frequency range and transformed into the susceptibility representation $\chi''_{NMR}(\omega) = \omega R_1(\omega)$. Three relaxation processes are identified, namely a main (α-) relaxation, a fast secondary (β-) relaxation and a slow relaxation; they are very similar for the two isomers. Exploiting frequency-temperature superposition, master curves of $\chi''_{NMR}(\omega\tau)$ are constructed and analyzed for the different processes. The α-relaxation displays a pronounced non-Lorentzian susceptibility with a temperature independent width parameter, and the correlation times display a non-Arrhenius temperature dependence – features indicating cooperative dynamics of the overall reorientation of the molecules. The β-relaxation shows high similarity with secondary relaxations in structural glasses. The extracted correlation times well agree with those reported by other techniques. A direct comparison of FC NMR and dielectric master curves for CNCH yields pronounced difference regarding the non-Lorentzian spectral shape as well as the relative relaxation strength of α- and β-relaxation. The correlation times of the slow relaxation follow an Arrhenius temperature dependence with a comparatively high activation energy. As the α-process involves liquid-like isotropic molecular reorientation, the slow process has to be attributed to vacancy diffusion, which modulates intermolecular dipole-dipole interactions, possibly accompanied by chair-chair interconversion of the cyclohexane ring. However, the low frequency relaxation features characteristic of vacancy diffusion cannot be detected due to experimental limitations.

Introduction

The plastically crystalline (PC) phase, also known as rotator phase or orientationally disordered phase, is a mesophase in which molecules have centers of mass ordered in a lattice, but they are able to rotate around their lattice points, so they show dynamical orientational disorder. Often, in the case of rigid, globular molecules, their overall reorientation is isotropic as in a liquid, and analogously, the motion is cooperative as significant reorientation can only occur when the surrounding molecules reorient as well. Such crystals show low values of melt entropy (ΔS_m).[1,2,3] In addition to the overall reorientation, a slower translational motion may be found, which often is described by defect (or vacancy) diffusion.[4] Bypassing the transition to an orientationally ordered phase, the PC phase can be supercooled leading to a slow-down of the dynamics until, finally, the system gets arrested by cooling below the glass transition temperature, T_g. Thereby, a glassy crystal (GC) is formed characterized by static orientational disorder but positional order. Since the slow-down of reorientational dynamics shows features that resemble those observed in structural glass formers, PC phases are often considered as model systems for studying the glass transition phenomenon. Many such systems were investigated by a variety of different techniques, including calorimetry, dielectric spectroscopy, quasielastic neutron scattering, NMR spectroscopy and relaxometry.[5,6,7,8,9] A prominent example is constituted by cyclohexanol; the term "glassy crystal" was first proposed for its PC phase below T_g by Adachi *et al.*[10] and a large number of investigations were performed on both the PC and GC phases of this material.[6] Another important example is cyanoadamantane with its molecular rigidity and globular shape. In its PC phase, the molecular jumps occurring along the six directions in a cubic lattice need a certain extent of cooperativity to accommodate each jump.[11,12]

The situation is more involved in the case of non-rigid molecules, like cyanocyclohexane (CNCH, $C_6H_{11}CN$) and isocyanocyclohexane (iCNCH, $C_6H_{11}NC$) considered in the present study, which undergo chair-chair interconversion between conformers with the CN (NC) group in equatorial or axial position with respect to the cyclohexane ring.[13,14,15] Both compounds show a PC phase, which can be easily supercooled.[5,16,17,18,19] The melting temperature, T_m, of CNCH and iCNCH is 282 K[16] (285 K[18]) and 266 K[16] (280 K[18]), respectively, with an associated low entropy of fusion (ΔS_m = (13.8 ± 0.2) J K^{-1} mol^{-1} and ΔS_m = (13.7 ± 0.8) J K^{-1} mol^{-1}, for CNCH and iCNCH, respectively,[16] or ΔS_m = 12.75 J K^{-1} mol^{-1} and ΔS_m = 15.12 J K^{-1} mol^{-1}, for CNCH and iCNCH, respectively[18]), characteristic of PC phases.[1] On cooling the PC phase under atmospheric pressure a GC forms at 134±1 K for CNCH and at 130±1 K for iCNCH.[16,18] A transition to an ordered crystalline phase occurs only under high pressure or after extremely long annealing.[16,17,18,19]

As far as dynamics is concerned, dielectric measurements on the PC phase of CNCH identified a main relaxation (α-process) and a secondary relaxation (β-process) at higher frequencies and lower temperatures.[20,21] Various ^{2}H NMR methods were applied in the PC and GC phases of CNCH to study the main (α-) and secondary (β-) processes.[22,23] It was found that the molecular motion associated with the α-process involves molecules undergoing small and large angular jumps, thus resulting in a liquid-like isotropic reorientation. For the β-process, ^{2}H NMR line shape analysis indicated the occurrence of a spatially highly restricted motion. In the case of iCNCH, correlation times for the α-relaxation process were determined by dielectric spectroscopy[19,21] and enthalpy relaxation measurements.[18] Dielectric measurements also identified a secondary β-relaxation persisting below T_g.[21] Both α- and β-processes were found to be very similar for CNCH and iCNCH.[21] Above T_g, indication of another process, slower than the α one, was found for CNCH and iCNCH by dielectric spectroscopy (yet, reproducibility was low)[21] and for iCNCH by enthalpy

relaxation measurements,[18] which was ascribed to the chair-chair interconversion.[17] This motion was postulated to be associated to a weak step-like signal in the calorimetric diagram at 170 K for CNCH[16] and at 160 K for iCNCH.[18]

Here, we report on a ^{1}H field-cycling (FC) NMR relaxometry study of CNCH and iCNCH in their PC phases. The FC NMR technique gained new momentum with the availability of a commercial relaxometer since about 2000 (Stelar Spinmaster 2000)[24] and new homebuilt machines.[25,26] Thanks to the possibility of measuring the spin-lattice relaxation rate, $R_1(\omega)$, over a broad range of Larmor frequencies, FC NMR relaxometry is particularly suited for probing the spectral density in condensed matter, like liquids, liquid crystals, and polymer melts.[27,28,29] However, so far only few studies applied the technique for exploring the dynamics in PC phases.[12,30,31,32]

Proton spin-lattice relaxation is determined by the fluctuations of the magnetic dipole-dipole interaction, and intra- as well as intermolecular relaxation contributions to R_1 have to be considered.[33] As a consequence, ^{1}H relaxation also probes translational diffusion as demonstrated for liquids and polymer melts, for example.[27,28,34] Translational diffusion in liquids, following the Stokes-Einstein-Debye relations in fair approximation, is only slightly slower than molecular rotation.[33] However, in the case of PC phases one expects translational diffusion to be well separated from rotation, and ^{1}H FC NMR may reveal particularly suited for investigating it, in analogy with the analysis of ^{1}H longitudinal relaxation times in the rotating frame ($T_{1\rho}$) used in the past.[4,35,36,37] Indeed, ^{1}H FC NMR was successfully employed for determining the self-diffusion coefficient in the PC phases of succinonitrile and cyclohexane,[30] of three dimethyl butanols,[32] and of chloro-adamantane.[31] In the present study ^{1}H FC NMR relaxometry is applied over a large temperature range to get insight into dynamical processes in the PC phase of CNCH and iCNCH.

Experimental

Materials. CNCH (98 %) and iCNCH (98 %) were purchased from SIGMA Aldrich and used without further purification.

^{1}H FC NMR Relaxometry Measurements. ^{1}H R_1 values were measured on CNCH and iCNCH at frequencies between 0.01 and 30 MHz using two commercial SpinMaster 2000 (Stelar srl) relaxometers, one located in Bayreuth and one in Pisa. Non-pre-polarizing and pre-polarizing sequences[24] were used above and below 12 MHz, respectively, with polarizing and detection frequencies of 25.0 and 16.3 MHz, respectively. The switching time was about 3 ms. The sample was contained in a standard 10 mm NMR tube, degassed and flame sealed. The temperature, stabilized for at least 10 min before each measurement, was controlled with a Stelar VTC90 variable temperature controller. In all cases, a mono-exponential function well reproduced the magnetization trends as a function of the variable delay; errors on R_1 were ≤ 2%.

Analysis of 1H FC NMR relaxation spectra

The relaxation spectra are analyzed in terms of the susceptibility representation, $\chi''_{NMR}(\omega)$, of the spin-lattice relaxation rate, $R_1(\omega)$. Correspondingly, we re-write the Bloembergen-Purcell-Pound (BPP)-type equation as:[33,38]

$$\chi''_{NMR}(\omega) \equiv \omega R_1(\omega) = \omega K[J(\omega) + 4J(2\omega)] = K[\chi''(\omega) + 2\chi''(2\omega)] \qquad (1)$$

where $J(\omega)$ denotes the spectral density and K is the NMR coupling constant which is linked to the effective second moment of the homo-nuclear dipolar interaction.

For the main relaxation, assuming frequency-temperature superposition (FTS) to hold and ignoring a weak temperature dependence of K, one can construct master curves $\chi''_{NMR}(\omega a_\alpha)$ by

solely shifting the dispersion spectra measured at different temperatures by a factor $a_\alpha(T)$ along the frequency axis to achieve best overlap. In order to transform the shift factors $a_\alpha(T)$ into the correlation times $\tau_\alpha(T)$, the susceptibility displaying a maximum at a reference temperature is fit to Eq. 1 using a Cole-Davidson (CD) susceptibility

$$\chi''_{CD}(\omega) = \frac{sin[\beta_{CD} \arctan(\omega\tau_{CD})]}{[1+\omega^2\tau_{CD}^2]^{\beta_{CD}/2}} \quad (2)$$

The CD function, a phenomenological function devised to take into account a distribution of motional correlation times resulting in a non-exponential correlation function, is frequently applied to describe the reorientational dynamics in glass forming systems. The parameter β_{CD} (with $0 < \beta_{CD} \leq 1$) describes the asymmetric (high-frequency) broadening of the susceptibility peak. The time constant τ_{CD}, representing the upper cut-off correlation time, is connected to the correlation time for the molecular reorientation via the relationship $\tau_\alpha = \tau_{CD}\beta_{CD}$. We note that the ^{1}H relaxation rate contains both intra- and inter-molecular contributions. Whereas in PC phases the translational dynamics is usually well separated from the rotational dynamics, there is also an intermolecular relaxation reflecting reorientational dynamics (the so-called eccentricity effect).[39,40] Here, we assume that this relaxation contribution can be described by the same CD function.

For the relaxations faster and slower than the α-relaxation, although NMR susceptibility maxima are not observed, susceptibility master curves are built with respect to reference temperatures to determine shift factors. In the case of the slow process, correlation times are determined from the shift factors by fitting the susceptibility curve at the reference temperature to Eq. 1 using a Debye (Lorentzian) susceptibility (Eq. 2 with $\beta_{CD} = 1$), which corresponds to an exponentially decaying correlation function characterized by a single correlation time.

Results

The ^{1}H spin-lattice relaxation rate, R_1, was measured between 10 kHz and 30 MHz in the temperature range from 173 K to 282 K in the PC phase and at 288 K in the liquid phase for CNCH, and from 160 to 273 K in the PC phase and at 293 K in the liquid phase in the case of iCNCH; data are shown in Figure 1.

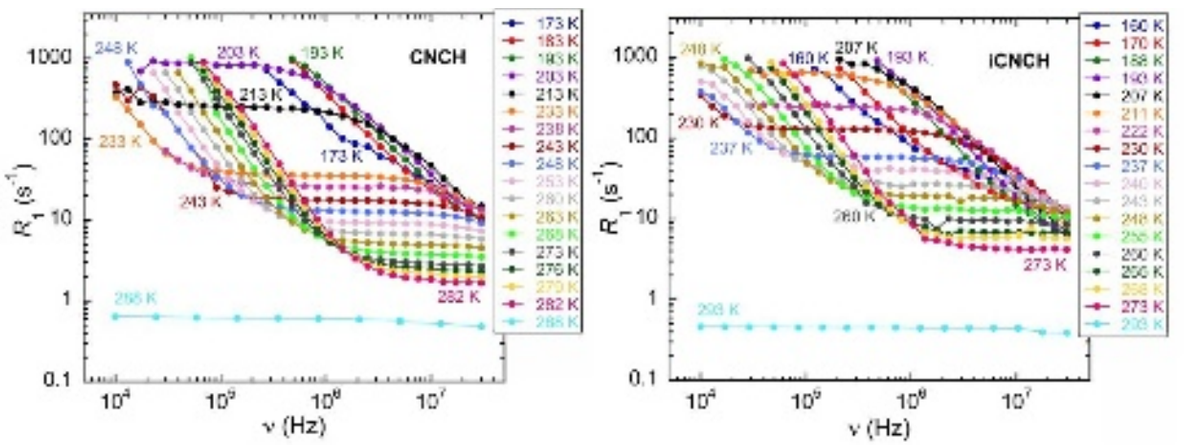

Figure 1. ^{1}H spin-lattice relaxation rate, R_1, of CNCH (left) and iCNCH (right) as a function of frequency measured by FC NMR relaxometry at the indicated temperatures. Lines are guides for the eye.

In the liquid phase, R_1 is essentially frequency-independent over the whole investigated frequency range indicating that dynamics is too fast to display dispersion effects in the frequency window of the relaxometer. In contrast, in the PC phase a strong dispersion is more or less visible at all temperatures and high frequency for both isomers, associated with the dynamics on the time scale of the reciprocal frequency. Passing to the susceptibility representation (Figure 2), an asymmetrically broadened $\chi''_{NMR}(\omega)$ peak is obtained, its maximum shifting out of the frequency window at higher temperatures. On the basis of previous dielectric and NMR data,[19,20,21,22,23] the

observed dispersions and corresponding $\chi''_{NMR}(\omega)$ peaks can be ascribed to the α-relaxation associated with the overall reorientation of the molecule.

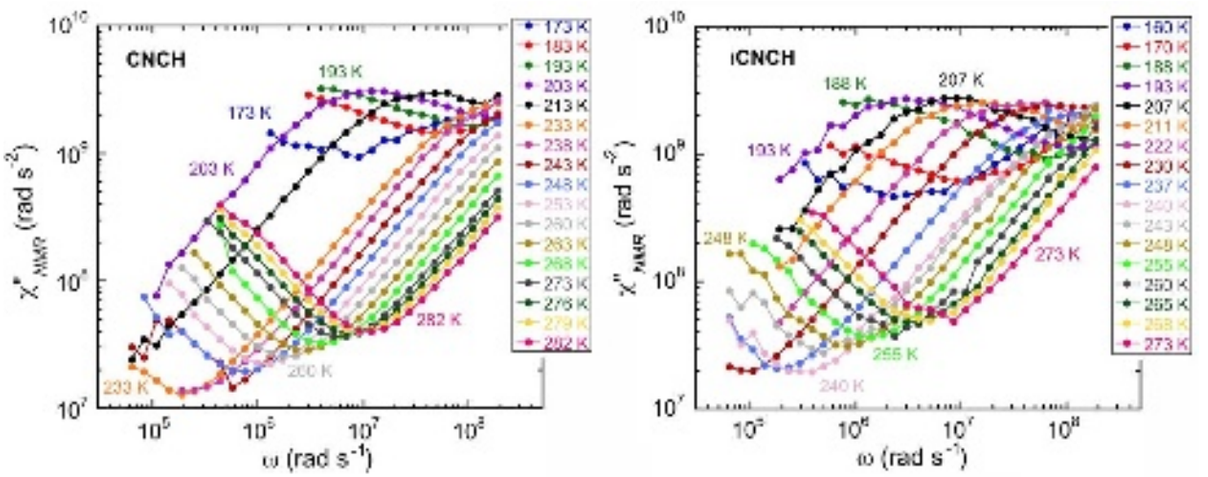

Figure 2. Relaxation data of CNCH (left) and iCNCH (right) at the indicated temperatures given in the susceptibility representation $\chi''_{NMR}(\omega) = \omega R_1(\omega)$ as a function of the angular frequency ω. Color code as in Figure 1. Lines are guides for the eye.

A second dispersion regime, corresponding to a slower dynamic process, is observed at low frequencies from 223 K or 230 K up to T_m for CNCH and iCNCH, respectively (Figure 1), which leads to another relaxation peak in the susceptibility representation, yet not fully covered by the accessible relaxation data (Figure 2) because R_1 reaches values exceeding the relaxometer limit determined by the switching time. Correspondingly, no plateau is observed for the R_1 dispersion at the investigated temperatures. The possible origin of this process will be addressed in Discussion and Conclusion.

Inspecting the relaxation data at high frequencies and low temperatures, in particular in the susceptibility representation (Figure 2), one finds indication of a third, fast relaxation process. We anticipate that this process can be identified as the β-relaxation reported in dielectric and ^{2}H NMR studies.[20,21,22,23]

As in the case of analyzing FC NMR data in liquids,[41] we first attempted to construct a master curve regarding the α-relaxation. The large spectral separation of this relaxation from the slow as well as from the fast relaxation contribution makes this attempt promising. As discussed above, building a master curve assumes FTS to hold, i.e., the spectral shape of the susceptibility remains the same while only its time constant changes with temperature. In the case of NMR relaxation data, we further assume that the temperature dependence of the coupling constant K can be ignored (cf. Eq 1). However, in the case of the occurrence of a β-relaxation with a relaxation strength increasing with temperature at the expense of that of the α-relaxation ($T > T_g$), as previously observed for CNCH,[20,42] the assumption of a constant relaxation strength (in addition to a non-changing spectral shape) is not strictly given. Anticipating the success of the master curve construction described below, it appears that this effect can be disregarded in the case of the FC NMR data.

Explicitly, the $\chi''_{NMR}(\omega)$ curves of Figure 2 were shifted solely along the frequency axis to achieve best overlap. The relaxation spectra at 203 K and at 211 K for CNCH and iCNCH, respectively, were taken to determine τ_α by fitting a CD function to the susceptibility spectrum. This allows to determine $\tau_\alpha(T)$ values from the shift factors $a_\alpha(T)$. For both samples an almost perfect overlap extending over about four decades in frequency is recognized encompassing relaxation data in the temperature range 173-282 K and 160-268 K for CNCH and iCNCH, respectively (Figure 3). The

part represented by the master curve reflects the susceptibility of the main reorientational dynamics and does not significantly differ for the two isomers. Very similar deviations from the master curves are found either: the master curve construction clearly fails at high temperatures and low frequencies due to the appearance of the low-frequency process, and at low temperatures and high frequencies due to a fast β-process.

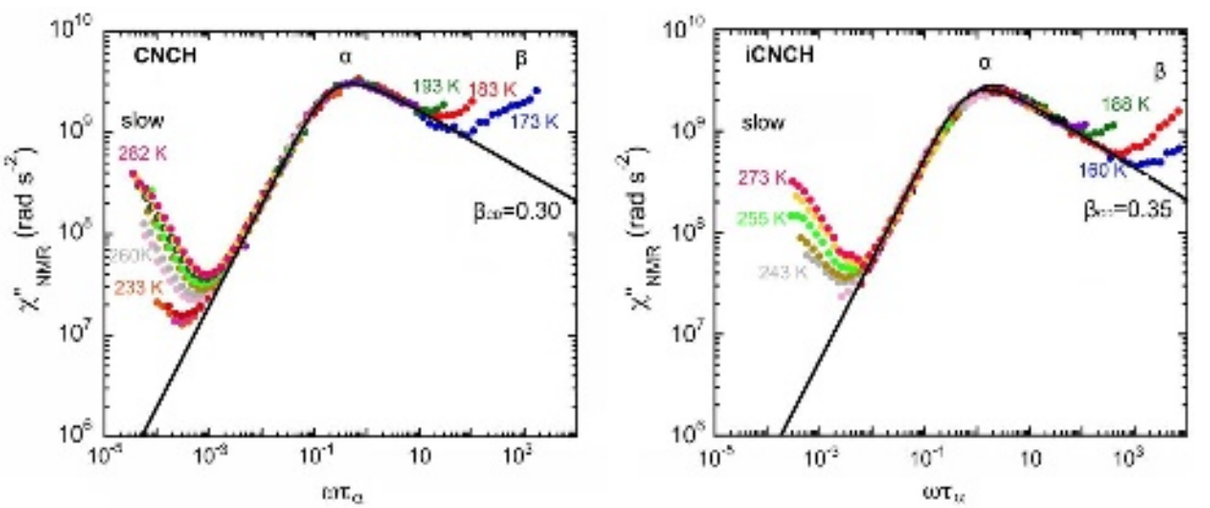

Figure 3. Susceptibility master curves for the α-relaxation in the PC phase of CNCH (left) and iCNCH (right); color code as in Figure 1. Black lines represent fits by applying a CD susceptibility (Eq. 2).

The strongly asymmetric spectral shape of the susceptibility master curves of CNCH and iCNCH is fitted by a CD function (Eq. 2). A very good fit is obtained with coupling constants K_α = 1.24 10^9 s^{-2} and K_α =9.61 10^8 s^{-2}, and β_{CD} =0.30 and β_{CD} =0.35 for CNCH and iCNCH, respectively. Constructing the master curves also yields $\tau_\alpha(T)$ - see Figure 4. The time constants of CNCH and iCNCH differ only slightly and are in good agreement with those previously determined by dielectric and ^{2}H NMR spectroscopy, which are included in Figure 4.[19,20,21] This justifies the

master curve construction a posteriori. The non-Arrhenius temperature dependences of the time constants can be interpolated by a Vogel-Fulcher-Tammann (VFT) equation

$$\tau_\alpha = \tau_0 exp\left(\frac{D}{T-T_\infty}\right) \quad (3)$$

with τ_0 = 1.58 10^{-14} s, D = 1650 K, and T_∞ = 88 K for CNCH and τ_0 = 3.98 10^{-14} s, D = 1700 K, and T_∞ = 85 K for iCNCH, corresponding to T_g (τ_α =100 s) values of 133.4 K and 132.9 K, respectively. From the trends of τ_α *vs* temperature a fragility index, m, defined as[43]

$$m = \left.\frac{-dlog\tau_\alpha}{d(T_g/T)}\right|_{T=T_g} = \frac{0.4342DT_g}{(T_g-T_\infty)^2} \quad (4)$$

is determined. Values of 46.5 and 42.7 are found for CNCH and iCNCH, respectively, close to literature values (m is 55.1 in ref. 20 and 49.5 in ref. 21 for CNCH, while it is 38 in ref. 19 and 40.1 in ref. 21 for iCNCH).

In order to definitely assign the fast relaxation to a β-relaxation, a master curve of $\chi''_{NMR}(\omega)$ was built for both isomers - again ignoring a possible changing relaxation strength. Since a maximum is not visible for this process at any of the temperatures investigated, only shift factors, $a_\beta(T)$, can be obtained with respect to the lowest investigated temperature (160 K for CNCH and 173 K for iCNCH). The $a_\beta(T)$ values display an Arrhenius temperature dependence with activation energy of about 20 kJ mol^{-1} for both isomers, which is similar to that previously reported for the time constants of the β-process, $\tau_\beta(T)$ (21.1 and 23.4 kJ mol^{-1} for CNCH and iCNCH, respectively).[20,21] The shift factors can be scaled to match $\tau_\beta(T)$ determined by dielectric spectroscopy[20,21] and by ^{2}H NMR[22,23] in the PC and GC phases, as shown in Figure 4.

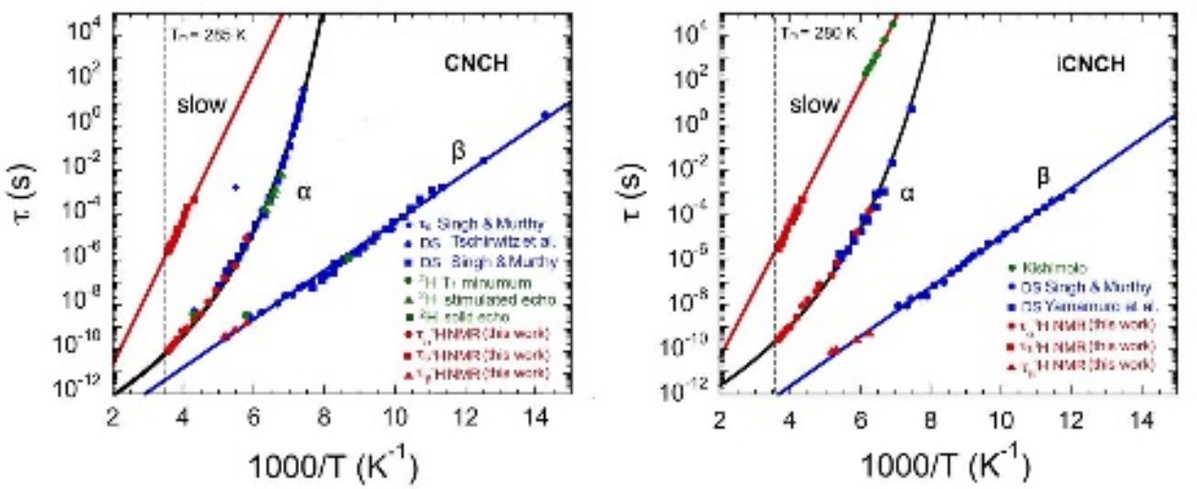

Figure 4. Correlation times for CNCH (left) and for iCNCH (right) determined for α-, β-, and slow relaxation processes by ^{1}H FC NMR relaxometry in the present work (red symbols) and by DS (blue symbols)[19,20,21] and ^{2}H NMR (green symbols)[22,23] in previous works. The black lines represent fits of $\tau_\alpha(T)$ to the VFT equation (Eq. 3). The blue and red lines represent Arrhenius laws fitting $\tau_\beta(T)$ and $\tau_s(T)$, respectively.

Next we turn to the analysis of the slow relaxation observed at low frequencies and high temperatures. Even though a maximum of $\chi''_{NMR}(\omega)$ is not observed, one recognizes in Figure 2 a high-frequency flank of the susceptibility peak depending on frequency as ω^{-1} at all the investigated temperatures ≥ 233 K and ≥ 230 K for CNCH and iCNCH, respectively. Thus, again master curves are constructed for data above 248 K taking the curve at the highest temperature (282 K for CNCH and 273 K for iCNCH) as reference (Figure 5) and shift factors, $a_s(T)$, are determined. The incomplete observation of a susceptibility peak hampers a detailed testing for a relaxation contribution arising, for instance, from translational diffusion (see Discussion and Conclusion). However, there is some change in the $\chi''_{NMR}(\omega)$ slope in the data at lowest

frequencies indicating an incipient relaxation maximum. Thus, an estimate of the time constants τ_s can be obtained by fitting the susceptibility curves with a simple Debye susceptibility (Eq. 2 with $\beta_{CD} = 1$), which well reproduces the ω^{-1} dependence of the high frequency flank of $\chi''_{NMR}(\omega)$ for the slow relaxation.

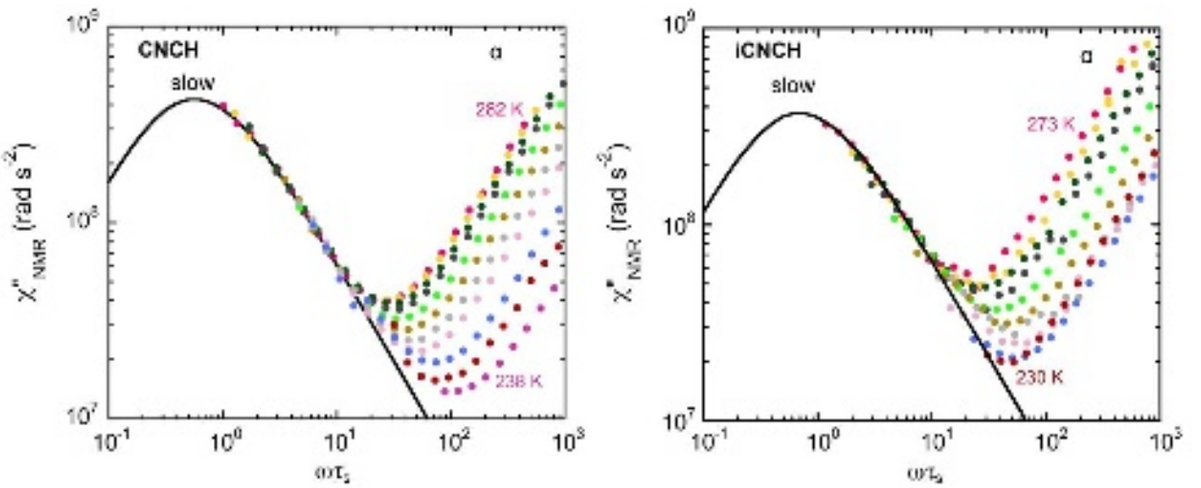

Figure 5. Susceptibility master curves for the slow relaxation process of CNCH (left) and iCNCH (right) observed at low frequencies and high temperatures. Black lines represent calculated curves assuming a Debye susceptibility. The increasing susceptibility values at high frequencies are ascribed to the α-relaxation.

As shown in Figure 5, good interpolation is obtained with effective coupling constants K_s = 7.5 10^7 s^{-2} and K_s =7.0 10^7 s^{-2} for CNCH and iCNCH, respectively, 14-17 times lower than those found for the α-relaxation, and τ_s values ranging from 10^{-6} to 10^{-4} s (Figure 4). The correlation times are quite similar for the two isomers and their temperature dependence can be well described by an Arrhenius equation with activation energy of 62 ± 3 and 63 ± 3 kJ mol^{-1} for CNCH and iCNCH, respectively. The activation energy values are not much different from that of a "slow process"

reported by a calorimetric study for iCNCH (51 kJ mol^{-1}), yet, measured at much lower temperature.[18] The corresponding time constants, included in Figure 4, and the present $\tau_s(T)$ for iCNCH can be well interpolated by a common Arrhenius law with an activation energy of 58 kJ mol^{-1}. We will come back to this point in Discussion and Conclusion.

In order to crosscheck the validity of the assumptions made in our analysis for the α-relaxation and the slow relaxation, $\tau_\alpha(T)$ and $\tau_s(T)$ (Figure 4), β_{CD}, K_α, and K_s values were used to reproduce the susceptibility spectra in the frequency region where the two processes dominate relaxation by assuming additivity of their contributions in terms of relaxation rates. As shown in Appendix (Figure 8), a good reproduction of the experimental susceptibilities is achieved, except at high frequencies and low temperature where the contribution of the β-process interferes. Satisfactory agreement between experimental and calculated data can also be seen by looking at the temperature dependence of R_1 at different frequencies reported in Figure 6. We added to Figure 6 ^{2}H longitudinal relaxation data taken at 46.07 MHz for CNCH,[22,23] which well fit into the frequency evolution of ^{1}H $R_1(T)$ after appropriately scaling the amplitude. As much lower temperatures are covered by ^{2}H R_1 measurements, a second maximum is well recognized attributed to the β-process. Remarkably, the amplitude of the β-relaxation is comparable to that of the α-process.

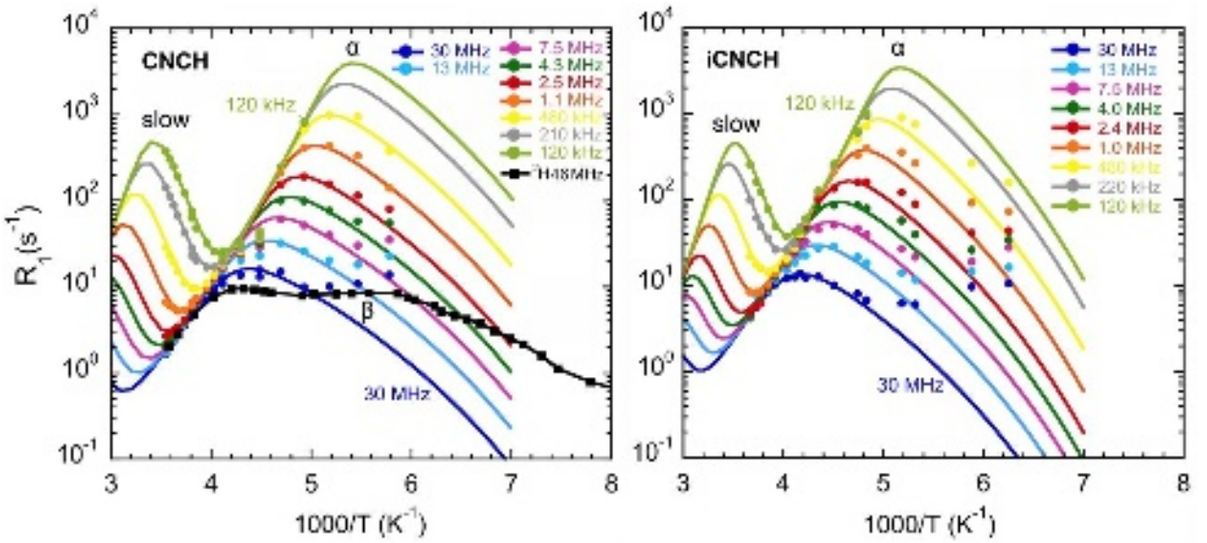

Figure 6. ^{1}H spin-lattice relaxation rate R_1 at different Larmor frequencies (colored symbols) as a function of inverse temperature for CNCH (left) and iCNCH (right). Colored lines indicate ^{1}H R_1 back calculated with the parameters obtained by the master curve analyses for the α- (R_1 maximum on the right) and the slow relaxation processes (R_1 maximum on the left), see text. For comparison, ^{2}H R_1 values measured at 46.07 MHz on CNCH[22] (black symbols and line) are added, scaled in amplitude. In this case, the maximum on the left is ascribed to the α-relaxation, while that on the right is due to the β-relaxation.

Discussion and Conclusion

Covering a large temperature range, ^{1}H FC NMR relaxometry allowed information to be collected on the evolution of the spectral density/susceptibility in the PC phase of the two isomers CNCH and iCNCH. In addition to a main (α-) relaxation, a faster secondary (β-) relaxation and a slower relaxation were identified. The α-relaxation obeys FTS and displays a pronounced non-Lorentzian susceptibility. The corresponding correlation times are very similar for the two isomers, agree with those reported by other techniques, and show a non-Arrhenius temperature dependence,

a feature well established for glass forming systems signaling cooperative dynamics. The temperature dependences of the correlation times of CNCH and iCNCH on approaching the glass transition are in the intermediate-to-strong fragility regime of Angell's classification scheme, as often observed for PC phases.[6,9] Regarding the β-relaxation, assuming again FTS and a constant relaxation strength, an activation energy close to that reported by dielectric and ^{2}H NMR spectroscopy is revealed.[20,21,22,23] This suggests that the increase of relaxation strength observed by dielectric spectroscopy for CNCH ($T > T_g$)[20] is not discernible in the NMR susceptibility.

In order to further dwell on the difference of the susceptibility as revealed by FC NMR and dielectric spectroscopy (data taken from ref. 20) the master curves normalized by re-scaling the main relaxation in each case are shown in Figure 7. Mere visual inspection discovers several differences. (i) The susceptibility maximum of the α-relaxation is significantly more asymmetric in the case of NMR. An interpolation with a CD function yields β_{CD}=0.30 and 0.35 for CNCH and iCNCH, respectively, whereas the dielectric spectra of CNCH give β_{CD}=0.60 at comparable temperatures, and some further broadening is observed at lower temperatures (not shown).[20] Possibly, the parameter β_{CD} of the NMR spectrum is underestimated somewhat due to the interference of the β-relaxation. (ii) The relaxation strength of the high-frequency β-process appears to be significantly smaller in the dielectric susceptibility. In the case of the NMR data, its amplitude is comparable in height to the main relaxation. This is confirmed by the ^{2}H relaxation data included in Figure 6, which even display a distinct β-relaxation maximum as temperatures down to T_g are covered. Thus, not only the spectral shape of the main relaxation is different but also the relative strengths of α- and β-relaxations. Up to our knowledge, such strong differences are typically not observed in glass forming systems. Only recently systematic differences among the relaxation strengths determined by different methods in supercooled liquids were

discussed.[44,45,46] (iii) Indication of a low-frequency process displaying $\varepsilon''(\omega) \propto \omega^{-1}$ is also found in the dielectric spectrum, yet, at much lower temperature and with lower amplitude. In simple liquids such spectral feature is usually ascribed to ubiquitous ionic impurities. Probably because to this, Tschirwitz *et al*. recorded it only for a single temperature and it was not mentioned in their paper.[20]

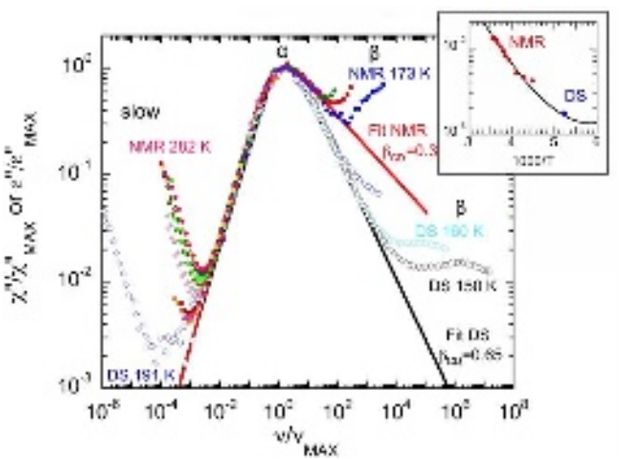

Figure 7. Normalized susceptibility master curves of the α-relaxation as obtained by ^{1}H FC NMR relaxometry (χ''/χ''_{MAX}, filled circles) and by dielectric spectroscopy ($\varepsilon''/\varepsilon''_{MAX}$, open diamonds). Interpolations of χ''/χ''_{MAX} (red line) and $\varepsilon''/\varepsilon''_{MAX}$ (black line) with a CD susceptibility with β_{CD} values as indicated. Data at lower reduced frequencies arise from the slow relaxation, those at higher frequencies from the β-relaxation. Inset: intensity at minimum between α-relaxation and slow relaxation in χ''/χ''_{MAX} (red symbols) and $\varepsilon''/\varepsilon''_{MAX}$ (blue symbol) curves as a function of inverse temperature; solid line represents trend expected from the FC NMR data (cf. text).

We note that Singh and Murthy reported indication of a slow dielectric-active process in CNCH,[21] yet, its amplitude was not reproducible and the corresponding time constant (τ_{slow}=0.0016 s at 185.6 K, also reported in Figure 4) does not fit to those determined here by FC NMR for the slow

process. A slow dielectric relaxation process with an activation energy of about 43 kJ/mol was reported for methyl cyclohexane in its liquid phase in addition to α- and β-relaxation.[47] The dielectric spectra by Tschwirtz et al.[20] reported in Figure 7 cover frequencies from 10^{-2} Hz to 30 MHz and thus probe the main relaxation peak at lower temperatures compared to FC NMR relaxometry. At such low temperatures the slow process identified by FC NMR is too slow to be routinely accessed by dielectric spectroscopy - if dielectrically active. Still, we can test whether this process "fits" to the NMR relaxation spectrum. Explicitly, after scaling both main relaxations to the same maximum (cf. Figure 7) we consider the amplitude of the relaxation minimum between the α- and the slow relaxation peaks as a function of temperature (see inset of Figure 7). The dielectric data point appears to follow the expectation trend given by the FC NMR data. The latter can easily be estimated from the temperature dependence of the respective time constants and from the known power-law character of the α-relaxation low-frequency flank and slow relaxation high-frequency flank. This comparison assumes that the relative relaxation strength of both processes is the same in both techniques and that the electric polarization is not fully relaxed by the main α-process. Accepting this, one may also expect a corresponding relaxation step in the real part, $\varepsilon'(\omega)$. However, such step cannot be identified in the present data, possibly because of its low amplitude. For example, assuming chair-chair interconversion as done in Ref. 18, the dipole moments of the equatorial conformer (3.7 D) and axial conformer (3.51 D)[21] differ only slightly and one may estimate a corresponding relaxation strength of about 5% of that of the α-relaxation. All in all, given a single dielectric spectrum any definite conclusion remains elusive.

Focusing solely on the spectral density (or susceptibility) as done by FC NMR relaxometry (and dielectric spectroscopy), no definite answer regarding the nature of the relaxation processes can be given. Yet, previous ^{2}H NMR investigations on CNCH clearly demonstrated that the α-process

can be ascribed to an overall isotropic reorientation of the molecules averaging the full quadrupolar interaction to zero at high temperatures.[22,23] Small and large angular jumps occur concurrently, a similar situation as for molecular reorientation in viscous liquids. This is in contrast to cyanoadamantane for which the cubic lattice symmetry induces a well-defined six-fold jump process by 90°.[11,12] Concerning the β-relaxation, ^{2}H NMR line-shape experiments[22,23] revealed very similar spectral features, as found for the secondary relaxation process in structural glasses like toluene, for example[48,49]. A "wobbling in a cone" model well describes ^{2}H NMR spectra.[22,23] Neglecting any collective effects, one can expect that the relaxation strength of such spatially highly restricted motion is by a factor of three larger in the NMR susceptibility than in the dielectric spectra due to the different rank of the Legendre polynomial correlation functions involved.[50,51,52] Yet, it appears that this cannot account for the large difference in the relative strength of the β-process as observed by the two methods (cf. Figure 7).

As far as the slow process is concerned, its susceptibility high-frequency flank follows a Lorentzian spectral shape and the correlation times follow an Arrhenius law with a rather high activation energy of 62 kJ mol^{-1} and 63 kJ mol^{-1} for CNCH and iCNCH, respectively. This activation energy is not far from 51 kJ mol^{-1} reported for a slow relaxation process of iCNCH in a calorimetric study of Kishimoto et al.,[18] yet, at much lower temperatures. Indeed, a linear interpolation of the two data sets suggest that the same process could be probed by NMR and calorimetry (see Figure 4). As possible origin, literature[18,21] discusses chair-chair interconversion exchanging equatorial and axial position of the molecule's protons (and substituents), which is documented for cyclohexane,[53] CNCH and iCNCH[17] in the PC phase, as well as for CNCH and iCNCH in solution.[14,15,54] Also the mentioned slow relaxation in liquid methylcyclohexane was attributed to such interconformational change.[47] By NMR techniques, McGrath and Weiss

identified the chair-chair interconversion in the PC phase of cyclohexane; they reported an activation energy of about 45 kJ mol^{-1}.[53] In the case of the present systems one expects a higher value due the voluminous CN group attached to the aliphatic ring. In solution the chair-chair interconversion of CNCH shows an activation energy of 46 kJ mol^{-1}.[54] In the PC phase chair-chair interconversions are expected to be of cooperative nature as one conformational change has to be accompanied by that of neighboring molecules in order to accommodate the atom´s new positions. Actually, McGrath and Weiss were not able to fully explain both the ^{2}H and ^{1}H spectra of cyclohexane in the PC phase and stated that the time scale of the conformational process suggests a mechanistic correlation with translational diffusion. As already mentioned, one expects also a dielectric loss accompanying chair-chair transitions.

Here, one has to stress that the slow relaxation as probed by FC NMR must reflect intermolecular dynamics, for example vacancy diffusion - as discussed in other NMR studies on PC phases.[4,30,31,32,35,36,37] Proton relaxation is dominated by fluctuations of the magnetic dipole-dipole interaction, which through an intermolecular pathway can probe translational dynamics, whereas the intramolecular pathway reflects solely molecular reorientation. In the case of liquids, recently this has been successfully applied to determine the diffusion coefficient $D(T)$.[55] As the main (α-) process in the present systems involves isotropic reorientations, as proven by ^{2}H NMR,[22,23] the intramolecular dipole-dipole interaction is averaged to zero. Thus, the only remaining interaction has to be of intermolecular nature and can only be relaxed by translational motions. Hence, although the full susceptibility, and, in particular, its low-frequency square root dispersion law characteristic of three-dimensional diffusion[56] is not covered by the present measurements, we can conclude that the slow process clearly identified by ^{1}H FC NMR involves translational dynamics.

A direct way of demonstrating the relevance of intermolecular relaxation is given by performing isotope dilution experiments, i.e., diluting the protonated species by its deuterated counterpart.[28] This suppresses the intermolecular relaxation contribution. Such approach was taken by Stapf and Kimmich in the case of cyclohexane,[30] and the extracted diffusion coefficients well agreed with those derived from field gradient NMR experiments. In the Appendix (Figure 9), we re-plotted the cyclohexane ^{1}H relaxation data in the susceptibility representation clearly showing the expected decrease in the relaxation amplitudes upon isotopic dilution, thus indicating the intermolecular nature of the relaxation in cyclohexane. The comparison of cyclohexane data with those on CNCH (Figure 9) shows a similar behavior for the main and slow relaxations of the three systems, although both processes are faster for cyclohexane, thus again suggesting an intermolecular origin also for the slow process of CNCH and iCNCH.

One has to keep in mind that translational diffusion in crystals is usually accompanied by molecular reorientation or possibly by conformational changes in the case of the present systems. For example, as proven by ^{2}H NMR, crystalline benzene reorients between four directions, which reflect the four sites in the unit cell of the benzene crystal between which the molecule jumps.[57,58].

Finally, we note that recent advances in instrumentation will offer FC NMR relaxometers which reach frequencies significantly below the current limit of the earth field.[25,26] They provide high potential for future FC NMR relaxometry studies investigating slow dynamics in condensed matter. However, in the present case of characterizing the slow dynamics in fully protonated CNCH or iCNCH, as well as in other PC phases,[59] it is not the limited frequency range covered by the commercial relaxometer but the too long switching time that hampers relaxation rates higher than about 1000 s^{-1} to be measured and thus hinders to cover the full susceptibility of the slow process (cf. Figure 1). Therefore, fully characterizing the spectral density of the slow relaxation

and its molecular nature involving translational diffusion and, probably, molecular reorientation remains a task to be address by different methods. In particular, concerning NMR methods, measurements of relaxation times in the rotating frame ($T_{1\rho}$) or relaxation times of dipolar order (T_{1D}) as a function of temperature may help. Yet, independently of this, it is a great challenge to understand the strong spectral differences revealed in the susceptibility measured by NMR and dielectric spectroscopy, respectively, regarding the main (α) and secondary (β) relaxation.

Appendix

In Figure 8 we present the interpolation of the susceptibility data by the model described in the main text. Except for high frequencies, for which the β-relaxation becomes relevant and its spectral evolution cannot easily be implemented, the approach well interpolates the susceptibility of the main relaxation and slow relaxation.

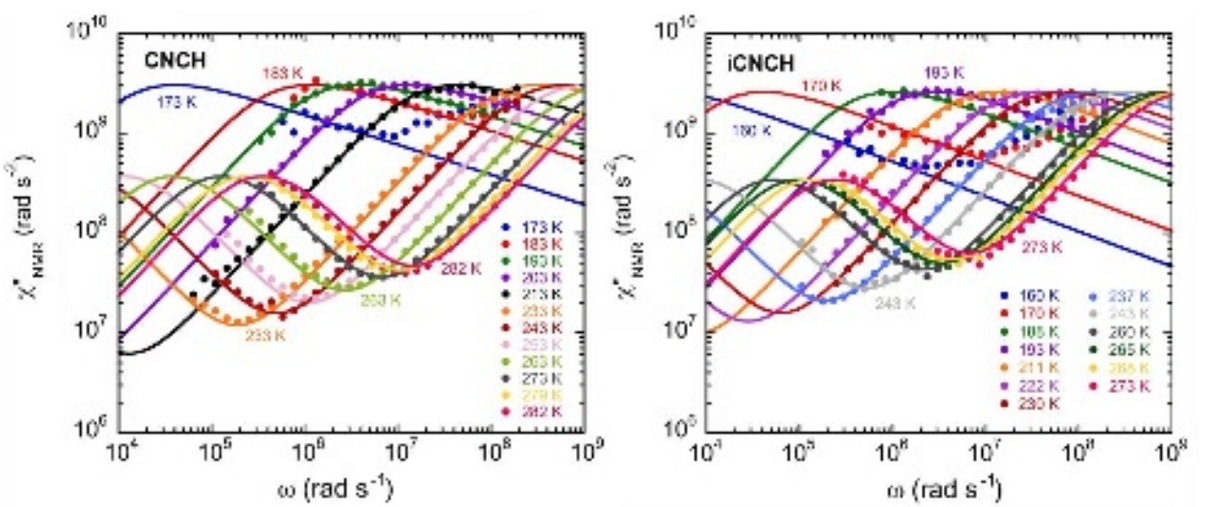

Figure 8. Relaxation data in the susceptibility representation for CNCH (left) and iCNCH (right) interpolated by the model function for both main and slow relaxations; see main text.

In Figure 9, we present ^{1}H relaxation data on cyclohexane taken by Stapf and Kimmich,[30] yet, plotted in the susceptibility representation. Clearly, the relaxation strength decreases strongly by mixing protonated cyclohexane with its deuterated counterpart, thus indicating the intermolecular nature of the relaxation. Traces of a main relaxation reflecting the overall rotation of the molecule[53] appear only at the highest frequencies. Compared with the corresponding data of CNCH, this suggests that the main relaxation and a possible intermolecular relaxation are shifted to lower frequencies for CNCH.

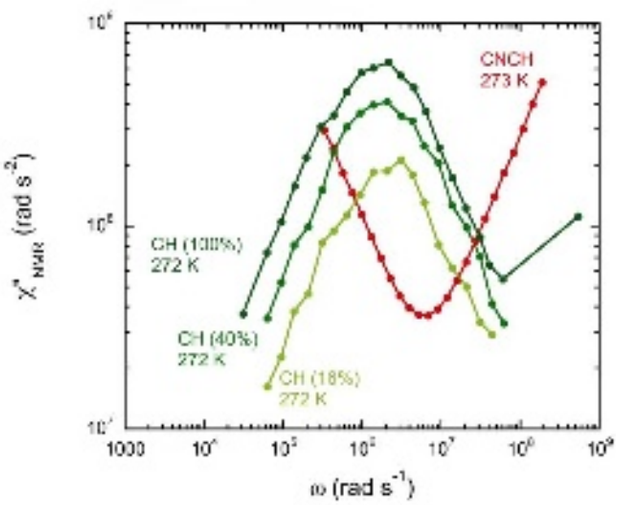

Figure 9. ^{1}H relaxation data of cyclohexane (CH) at different concentration in cyclohexane-d_6 in its PC phase at 272 K measured by Stapf and Kimmich[30] re-plotted in the susceptibility representation (green symbols); for comparison: present data of CNCH at 273 K (red symbols).

Author Contributions

The manuscript was written through contributions of all authors. All authors have given approval to the final version of the manuscript.

ACKNOWLEDGMENT

The authors would like to acknowledge the contribution of the COST Action 15209 (Eurelax: European Network on NMR Relaxometry) and of the CNR/PAS Italy/Poland 2020-2021 bilateral project. E.C. is grateful to the COST Action 15209 for supporting a short term scientific mission to Bayreuth University. E.A.R. appreciates the support of SFB 840.

DATA AVAILABILITY

The data that support the findings of this study are available from the corresponding authors upon reasonable request.

REFERENCES

[1] J. Timmermans, J. Phys. Chem. Solids **18**, 1 (1961).

[2] L. A. K. Staveley, Annu. Rev. Phys. Chem. **13**, 351 (1962).

[3] *The Plastically Crystalline State*. Sherwood, J. N., Ed.; John Wiley & Sons Limited, Chichester, New York, Brisbane, Toronto 1979.

[4] J. M. Chezeau and J. H. Strange, Phys. Rep. **53**, 1 (1979).

[5] H. Suga, Thermochim. Acta **245**, 69 (1994).

[6] R. Brand, P. Lunkenheimer, and A. Loidl, J. Chem. Phys. **116**, 10386 (2002).

[7] F. Affouard, J.-F. Willart, and M. Descamps, J. Non-Cryst. Solids **307-310**, 9 (2002).

[8] R. Böhmer, G. Diezemann, G. Hinze, and E. Rössler, Prog. Nucl. Magn. Reson. Spectrosc. **39**, 191 (2001).

[9] S. Benkhof, T. Blochowicz, A. Kudlik, C. Tschirwitz, and E. Rössler, Ferroelectrics **236**, 193 (2000).

[10] K. Adachi, H. Suga, and S. Seki, Bull. Chem. Soc. Jpn. **41**, 1073 (1968)

[11] S. A. Lusceac, I. Roggatz, P. Medick, J. Gmeiner, and E. A. Rössler, J. Chem. Phys. **121**, 4770 (2004).

[12] M. Flämig, N. Fatkullin, and E. A. Rössler, J. Chem. Phys. **151**, 224507 (2019).

[13] F. R. Jensen, C. Hackett Bushweller, and B. H. Beck, J. Am. Chem. Soc. **91**, 344 (1969).

[14] H-J. Schneider and V. Hoppen, J. Org. Chem. **43**, 3866 (1978).

[15] G. Corfield and M. Davies, Trans. Faraday Soc. **60**, 10 (1964).

[16] A. Gonthier-Vassal and H. Szwarc, Chem. Phys. Lett. **129**, 5 (1986).

[17] T. Woldbæk, A. Berkessel, A. Horn, and P. Klæboe, Acta Chem. Scand. A **36**, 719 (1982).

[18] I. Kishimoto, J-J. Pinvidic, T. Matsuo, and H. Suga, Proc. Japan. Acad. Ser. B **67**, 66 (1991).

[19] O. Yamamuro, M. Ishikawa, I. Kishimoto, J-J. Pinvidic, and T. Matsuo, J. Phys. Soc. Japan **68**, 2969 (1999).

[20] C. Tschirwitz, S. Benkhof, T Blochowicz, and E. Rössler, J. Chem. Phys. **117**, 6281 (2002).

[21] L. P. Singh and S. S. N. Murthy, J. Chem. Phys. **129**, 094501 (2008).

[22] B. Micko, S. A. Lusceac, H. Zimmermann, and E. A. Rössler, J. Chem. Phys. **138**, 074503 (2013).

[23] B. Micko, D. Kruk, and E. A. Rössler, J. Chem. Phys. **138**, 074504 (2013).

[24] R. Kimmich and E. Anoardo, Prog. Nucl. Magn. Reson. Spectrosc. **44,** 257 (2004).

[25] F. Fujara, D. Kruk, and A. Privalov, Prog. Nucl. Magn. Reson. Spectrosc. **82**, 39 (2014).

[26] B. Kresse, M. Becher, A. F. Privalov, M. Hofmann, E. A. Rössler, M. Vogel, and F. Fujara, J. Magn. Reson. **277**, 79 (2017).

[27] D. Kruk, A. Herrmann, and E. A. Rössler, Prog. Nucl. Magn. Reson. Spectrosc. **63**, 33 (2012).

[28] R. Meier, D. Kruk, and E. A. Rössler, ChemPhysChem **14**, 3071 (2013).

[29] R. Kimmich and N. Fatkullin, Prog. Nucl. Magn. Reson. Spectrosc. **101**, 18 (2017).

[30] S. Stapf and R. Kimmich, Mol. Phys. **92**, 1051 (1997).

[31] R. Decressain, L. Carpentier, E. Cochin, and J. P. Amoureux, Eur. Phys. J. B **58**, 223 (2007).

[32] E. Carignani, C. Forte, E. Juszyńska-Gałązka, M. Gałązka, M. Massalska-Arodź, A. Mandoli, M. Geppi, and L. Calucci, J. Phys. Chem. B **122**, 9792 (2018).

[33] A. Abragam, *The Principles of Nuclear Magnetism*; Clarendon Press: Oxford, UK, 1961.

[34] M. Flämig, M. Hofmann, N. Fatkullin, and E. A. Rössler, J. Phys. Chem. B **124**, 1557 (2020).

[35] S. B. W. Roeder and D. C. Douglass, J. Chem. Phys. **52**, 5525 (1970).

[36] N. Boden, J. Cohen, and R. T. Squires, Mol. Phys. **31**, 1813 (1976).

[37] S. M. Ross and J. H. Strange, J. Chem. Phys. **68**, 3078 (1978).

[38] S. Kariyo, C. Gainaru, H. Schick, A. Brodin, V. N. Novikov, and E. A. Rössler, Phys. Rev. Lett. **97**, 207803 (2006). Erratum: A. Herrmann, C. Gainaru, H. Schick, A. Brodin, V. N. Novikov, and E. A. Rössler, Phys. Rev. Lett. **100**, 109901 (2008).

[39] Y. Ayant, E. Belorisky, P. Fries, and J. Rosset, J. Phys. **38**, 325 (1977).

[40] R. Meier, D. Kruk, J. Gmeiner, and E. A. Rössler, J. Chem. Phys. **136**, 034508 (2012).

[41] M. Flämig, M. Hofmann, and E. A. Rössler, Mol. Phys. **117**, 877 (2019).

[42] A. Kudlik, C. Tschirwitz, T. Blochowicz, S. Benkhof, and E. Rössler, J. Non-Cryst. Solids **235-237**, 406 (1998).

[43] C. A. Angell, J. Non-Cryst. Solids **131-133**, 13 (1991).

[44] T. Körber, R. Stäglich, C. Gainaru, R. Böhmer, and E. A. Rössler, J. Chem. Phys. **153**, 124510 (2020).

[45] F. Pabst, A. Helbling, J. Gabriel, P. Weigl, and T. Blochowicz, Phys. Rev. E **102**, 010606 (2020).

[46] J. P. Gabriel, P. Zourchang, F. Pabst, A. Healbling, P. Weigl, T. Böhmer, and T. Blochowicz, Phys. Chem. Chem. Phys. **22**, 11644 (2020).

[47] A. Mandanici, W. Huang, M. Cutroni, and R. Richert, J. Chem. Phys. **128**, 124505 (2008).

[48] M. Vogel and E. Rössler, J. Phys. Chem. B **104**, 4285 (2000).

[49] M. Vogel and E. Rössler, J. Chem. Phys. **114**, 5802 (2001).

[50] M. J. Lebon, C. Dreyfus, Y. Guissani, R. M. Pick, and H. Z. Cummins, Z. Phys. B **103**, 433 (1997).

[51] T. Blochowicz, A. Kudlik, S. Benkhof, J. Senker, E. Rössler, and G. Hinze, J. Chem. Phys. **110**, 12011 (1999).

[52] A. Brodin, R. Bergman, J. Mattsson, and E. A. Rössler, Eur. Phys. J. B **36**, 349 (2003).

[53] K. J. McGrath and R. G. Weiss, Langmuir **13**, 4474 (1997).

[54] T. D. Phien, L. E. Kuzmina, A. Kvaran, S. Jonsdottir, I. Arnason, and S. A. Shlykov, J. Mol. Struct. **1168**, 127 (2018).

[55] D. Kruk, R. Meier, and E. A. Rössler, Phys. Rev. E **85**, 020201 (2012).

[56] C. A. Sholl, J. Phys. C: Solid State Phys. **14**, 447 (1981).

[57] T. Gullion and M. S. Conradi, Phys. Rev. B **32**, 7076 (1985).

[58] O. Isfort, B. Geil, and F. Fujara, J. Magn. Reson. **130**, 45 (1998).

[59] M. Flämig and E.A. Rössler, to be published.

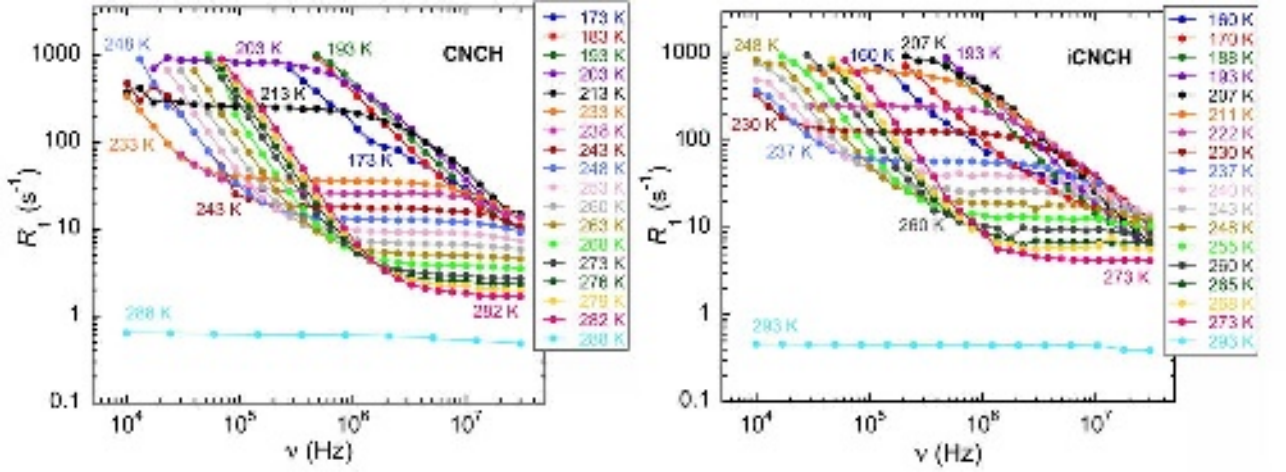
CNCH
iCNCH
R_1 (s^{-1})
ν (Hz)
1000
100
10
1
0.1
10^4
10^5
10^6
10^7
248 K
233 K
213 K
203 K
193 K
173 K
243 K
292 K
288 K
173 K
183 K
193 K
203 K
213 K
233 K
238 K
243 K
248 K
253 K
260 K
263 K
269 K
273 K
276 K
279 K
282 K
288 K
160 K
170 K
188 K
193 K
207 K
211 K
222 K
230 K
237 K
240 K
243 K
248 K
255 K
260 K
265 K
268 K
273 K
293 K

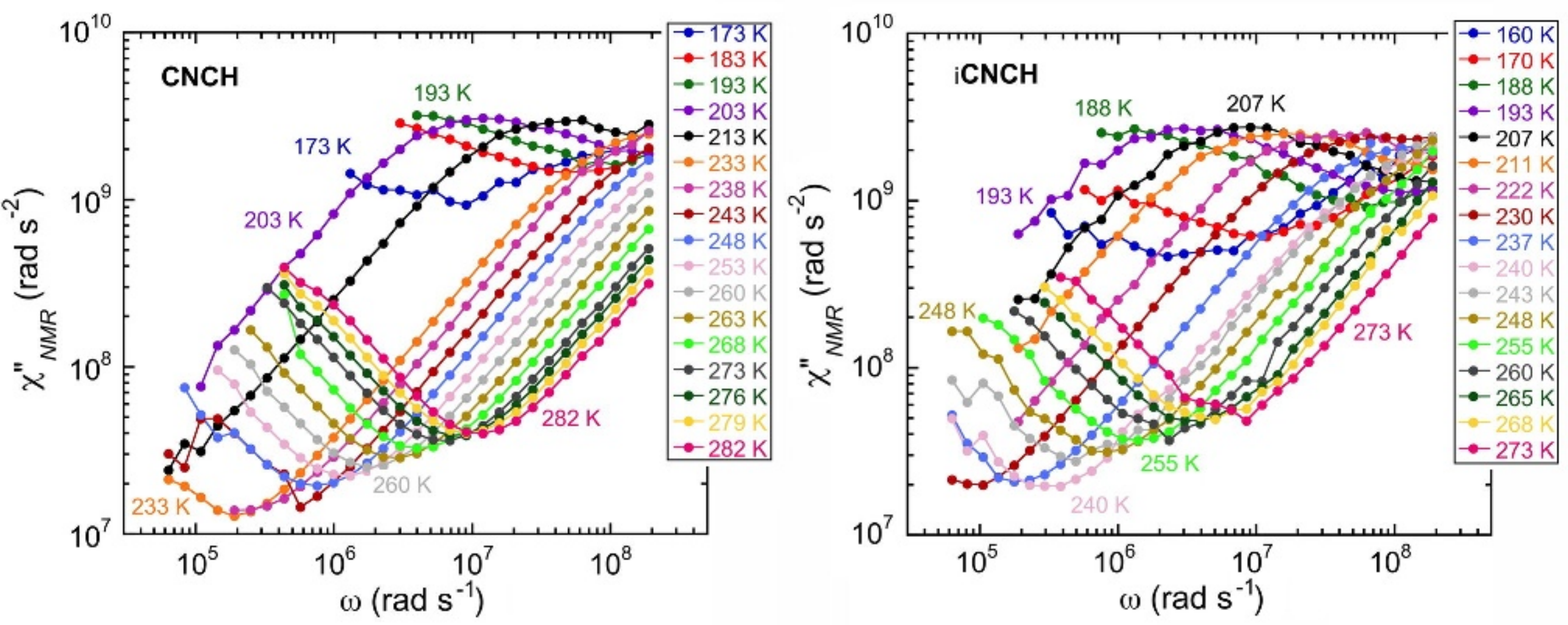
CNCH
iCNCH
χ"NMR (rad s-2)
ω (rad s-1)
173 K
183 K
193 K
203 K
213 K
233 K
238 K
243 K
248 K
253 K
260 K
263 K
268 K
273 K
276 K
279 K
282 K
160 K
170 K
188 K
193 K
207 K
211 K
222 K
230 K
237 K
240 K
243 K
248 K
255 K
260 K
265 K
268 K
273 K

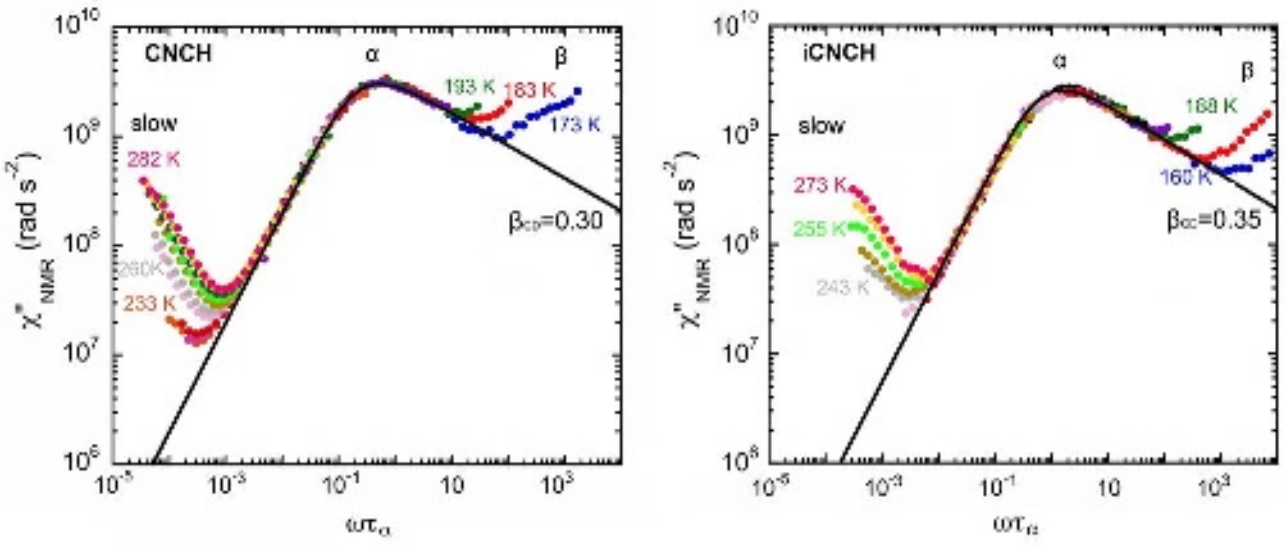
CNCH
α
β
slow
193 K
183 K
173 K
282 K
260K
253 K
β_{cp}=0.30
χ''_{NMR} (rad s^{-2})
$\omega\tau_\alpha$
iCNCH
168 K
160 K
273 K
255 K
243 K
β_{cc}=0.35

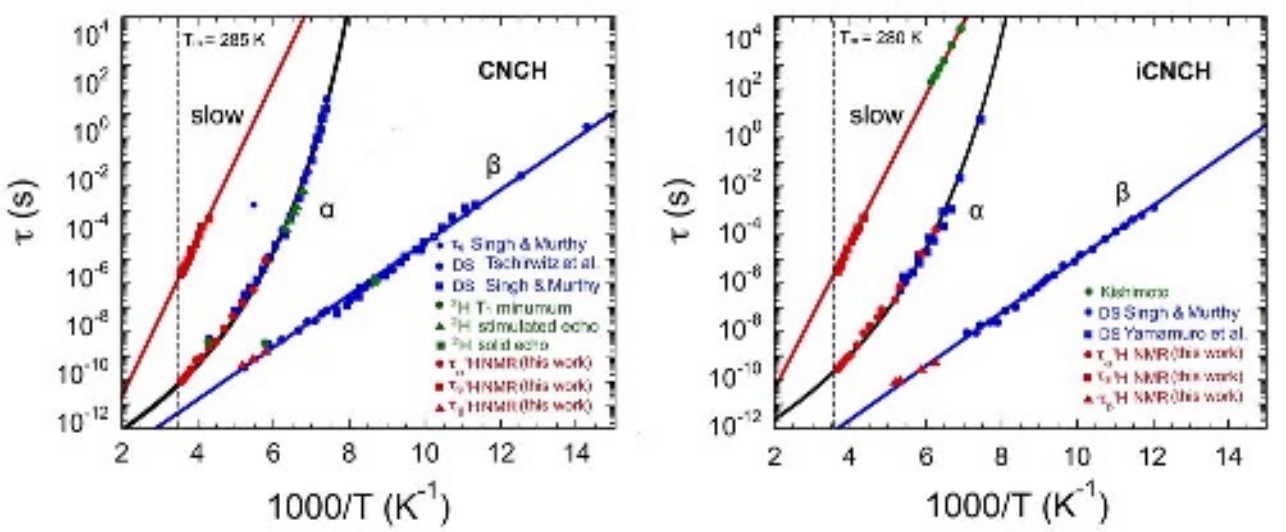
CNCH
iCNCH
slow
α
β
τ (s)
1000/T (K^{-1})
T_m = 285 K
T_m = 280 K
τ_α Singh & Murthy
DS Tschirwitz et al.
DS Singh & Murthy
^{2}H T$_1$ minimum
^{2}H stimulated echo
^{2}H solid echo
τ_α ^{2}H NMR(this work)
τ_β ^{2}H NMR(this work)
τ_β ^{2}H NMR(this work)
Kishimoto
DS Singh & Murthy
DS Yamamuro et al.
τ_α ^{2}H NMR(this work)
τ_β ^{2}H NMR(this work)
τ_β ^{2}H NMR(this work)

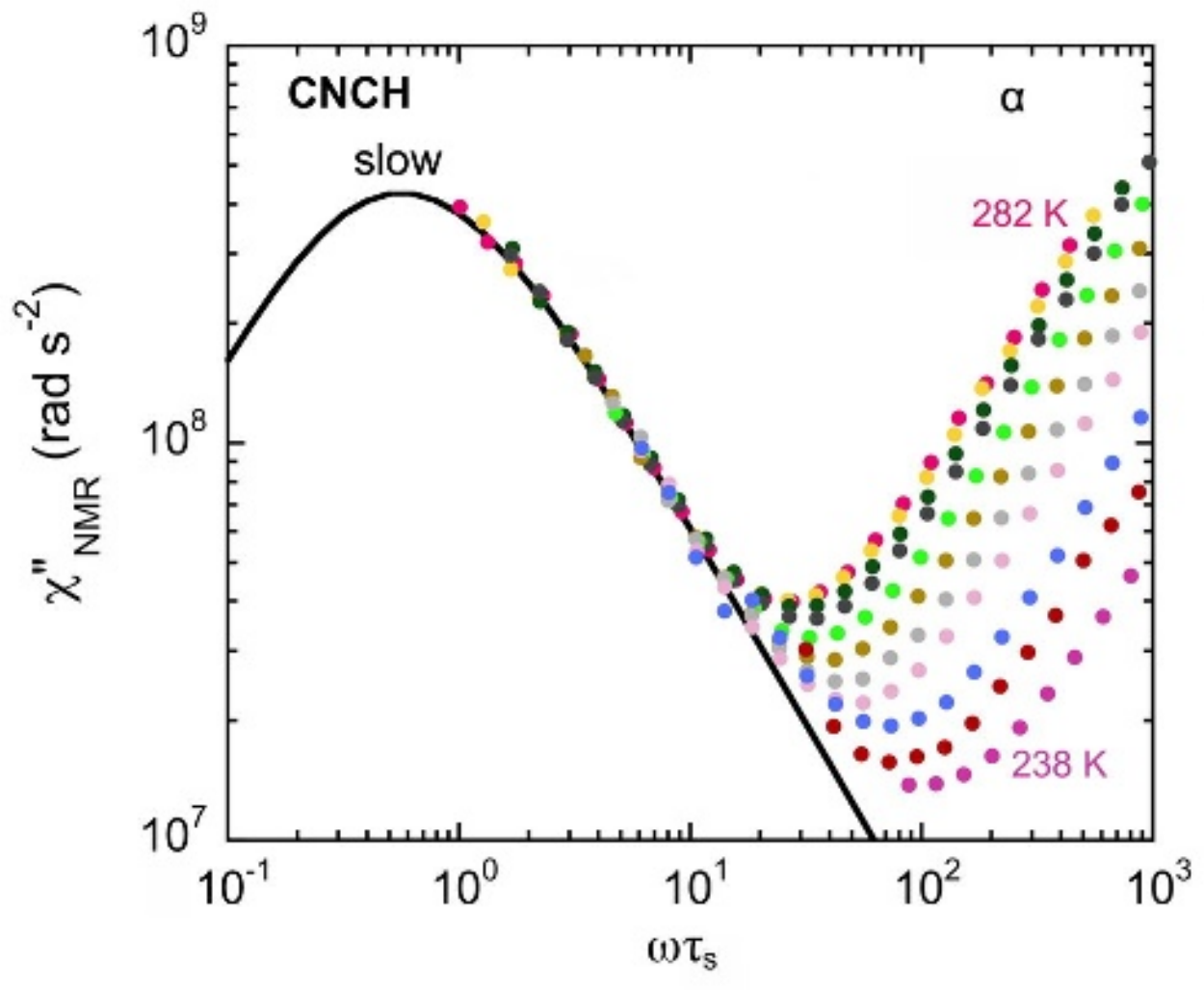
CNCH
α
slow
282 K
238 K
10^9
10^8
10^7
10^{-1}
10^0
10^1
10^2
10^3
χ''_{NMR} (rad s^{-2})
$\omega\tau_s$

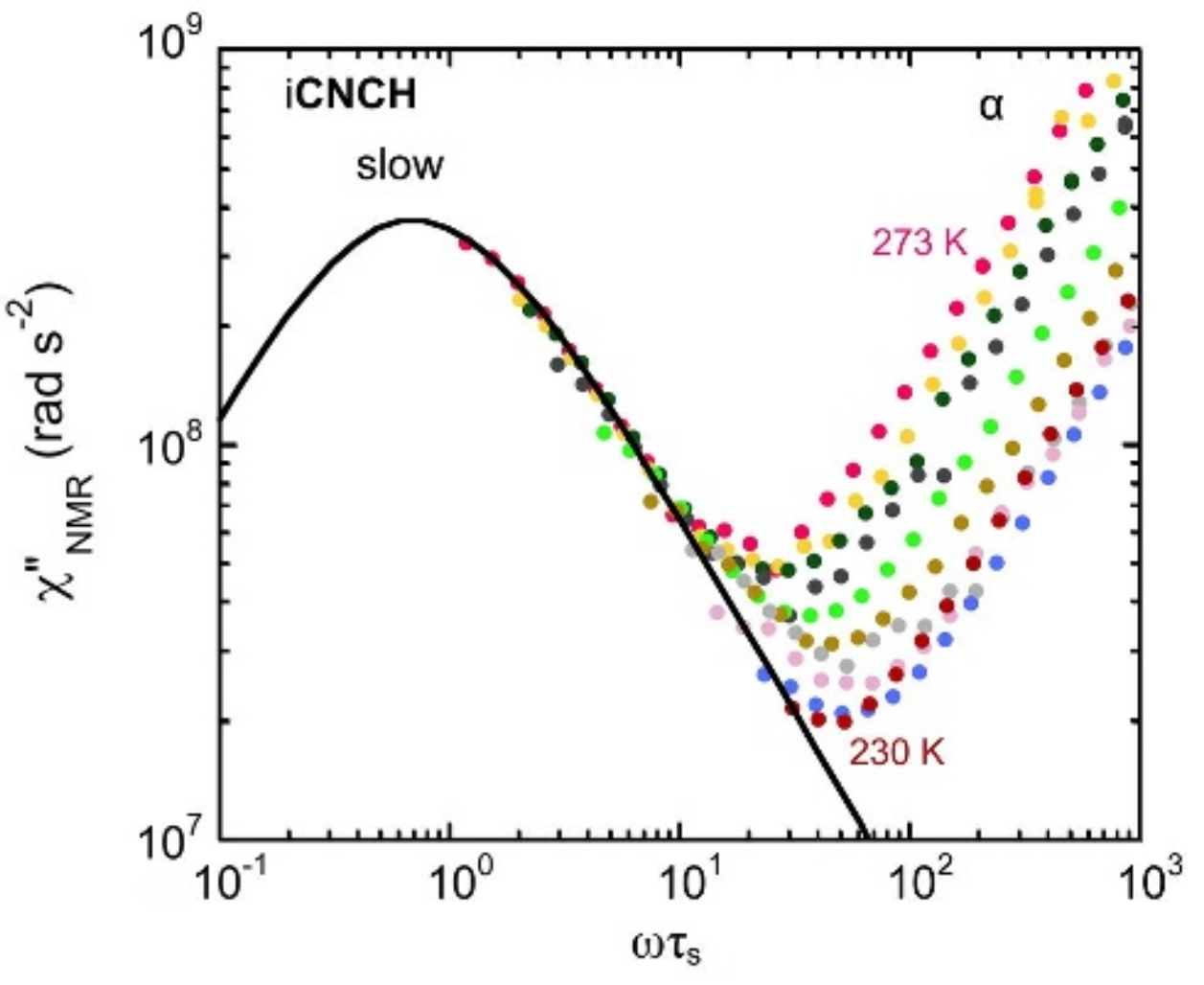
iCNCH
α
slow
273 K
230 K
10^9
10^8
10^7
10^{-1}
10^0
10^1
10^2
10^3
χ''_{NMR} (rad s^{-2})
$\omega\tau_s$

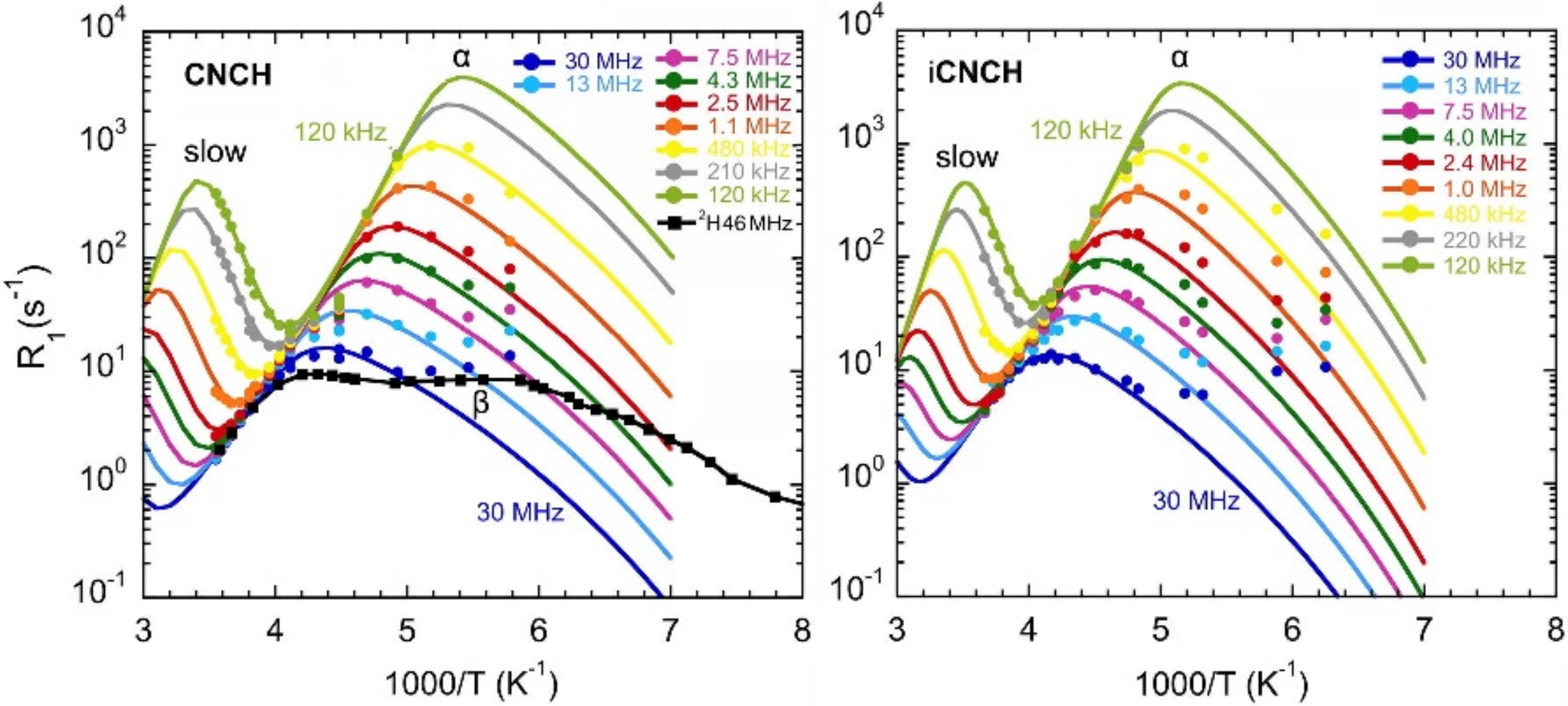
CNCH
α
β
slow
120 kHz
30 MHz
30 MHz
13 MHz
7.5 MHz
4.3 MHz
2.5 MHz
1.1 MHz
480 kHz
210 kHz
120 kHz
²H 46 MHz
R1 (s-1)
1000/T (K-1)
iCNCH
α
slow
120 kHz
30 MHz
30 MHz
13 MHz
7.5 MHz
4.0 MHz
2.4 MHz
1.0 MHz
480 kHz
220 kHz
120 kHz
1000/T (K-1)

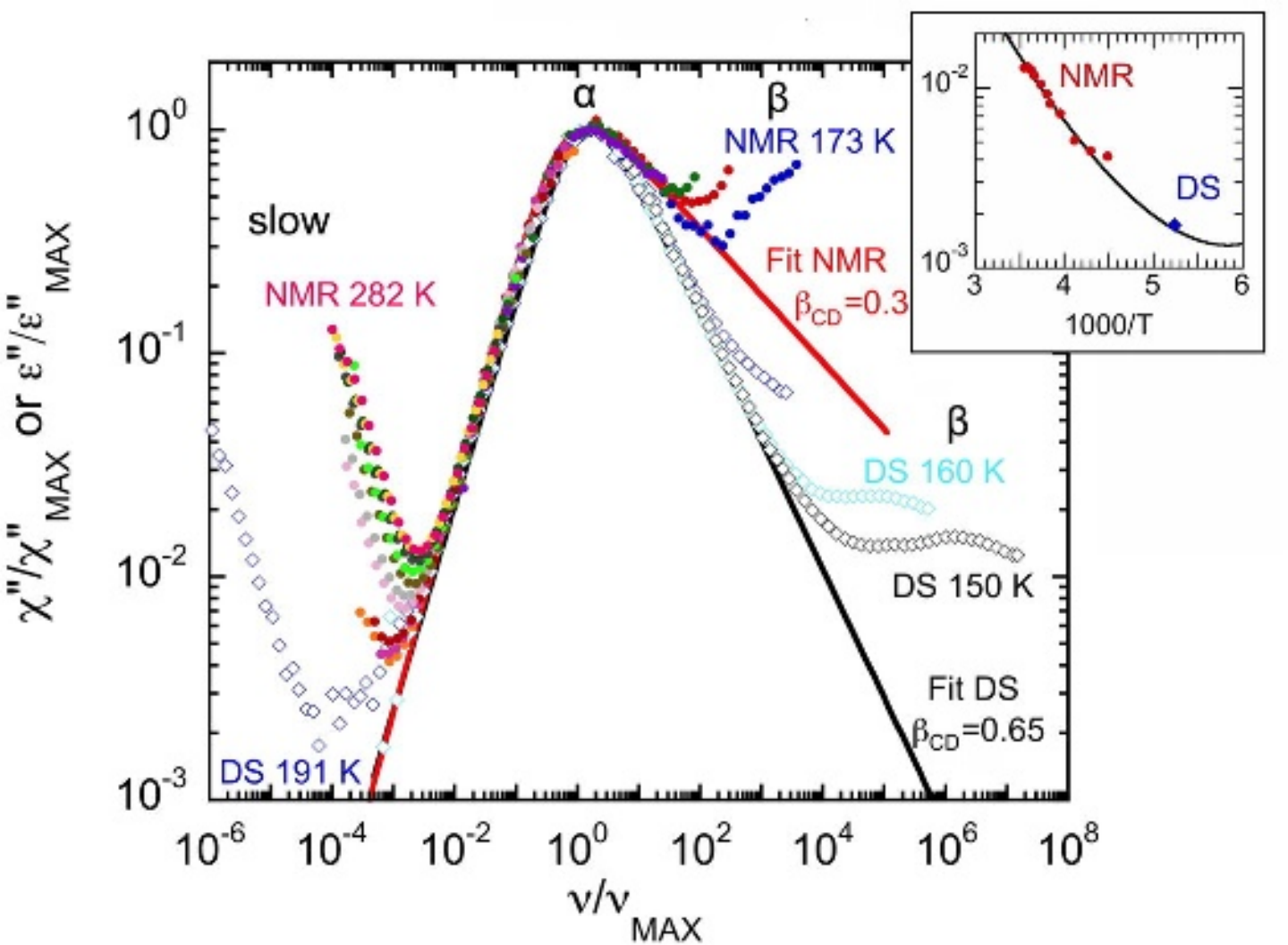
α
β
NMR 173 K
slow
NMR 282 K
Fit NMR
β_{CD}=0.3
β
DS 160 K
DS 150 K
Fit DS
β_{CD}=0.65
DS 191 K
χ''/χ''_{MAX} or $\varepsilon''/\varepsilon''_{MAX}$
ν/ν_{MAX}
10^{0}
10^{-1}
10^{-2}
10^{-3}
10^{-6}
10^{-4}
10^{-2}
10^{0}
10^{2}
10^{4}
10^{6}
10^{8}
NMR
DS
10^{-2}
10^{-3}
3
4
5
6
1000/T

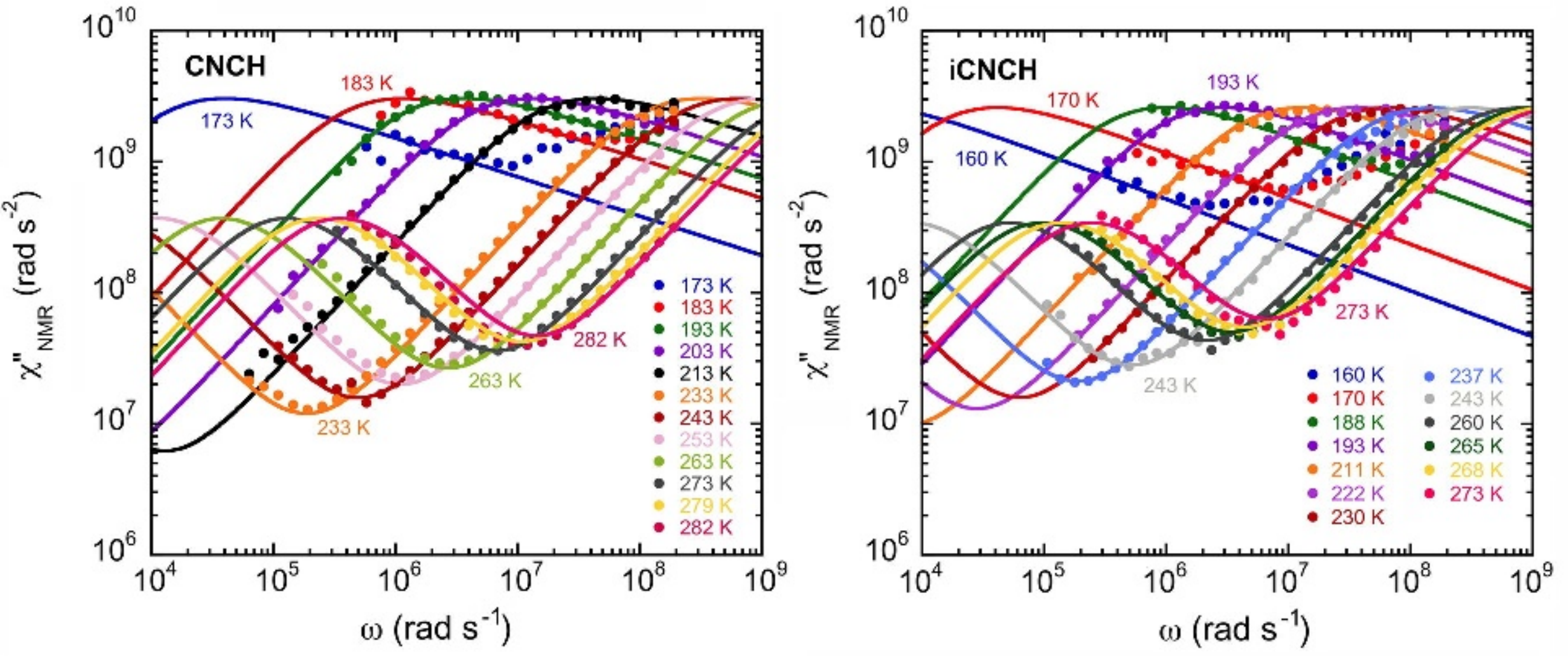
CNCH
183 K
173 K
282 K
263 K
233 K
173 K
183 K
193 K
203 K
213 K
233 K
243 K
253 K
263 K
273 K
279 K
282 K
χ''_{NMR} (rad s^{-2})
ω (rad s^{-1})
iCNCH
193 K
170 K
160 K
273 K
243 K
160 K
170 K
188 K
193 K
211 K
222 K
230 K
237 K
243 K
260 K
265 K
268 K
273 K
χ''_{NMR} (rad s^{-2})
ω (rad s^{-1})

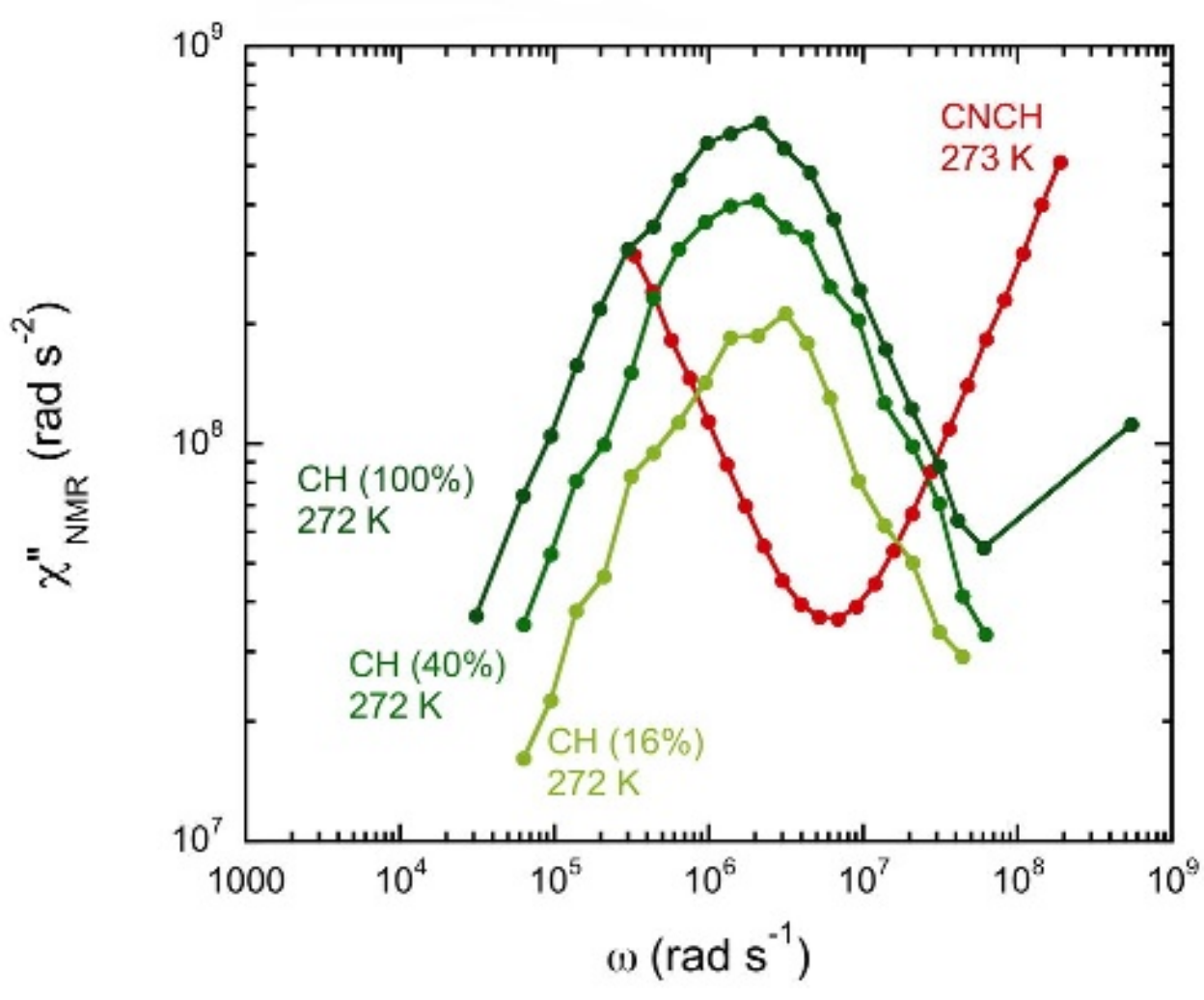
10^9
10^8
10^7
χ''_{NMR} (rad s^{-2})
CNCH
273 K
CH (100%)
272 K
CH (40%)
272 K
CH (16%)
272 K
1000
10^4
10^5
10^6
10^7
10^8
10^9
ω (rad s^{-1})